

Article pubs.acs.org/JACS

## Mechanistic Insight into the Stereoselective Cationic Polymerization of Vinyl Ethers

Travis P. Varner, Aaron J. Teator, Yernaidu Reddi, Paige E. Jacky, Christopher J. Cramer, and Frank A. Leibfarth\*



Cite This: J. Am. Chem. Soc. 2020, 142, 17175-17186



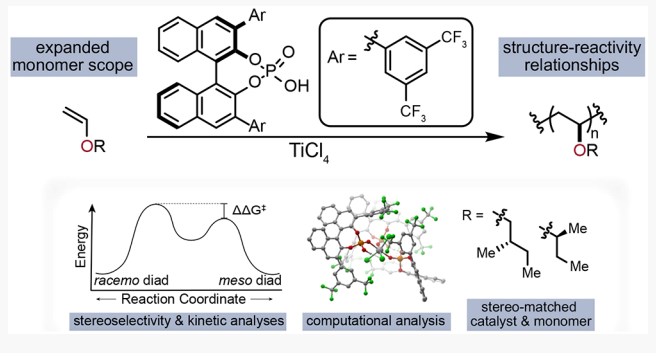
**ACCESS** I

III Metrics & More

Article Recommendations

Supporting Information

ABSTRACT: The control of the tacticity of synthetic polymers enables the realization of emergent physical properties from readily available starting materials. While stereodefined polymers derived from nonpolar vinyl monomers can be efficiently prepared using early transition metal catalysts, general methods for the stereoselective polymerization of polar vinyl monomers remain underdeveloped. We recently demonstrated asymmetric ion pairing catalysis as an effective approach to achieve stereoselective cationic polymerization of vinyl ethers. Herein, we provide a deeper understanding of stereoselective ion-pairing polymerization through comprehensive experimental and computational studies. These findings demonstrate the importance of ligand deceleration



effects for the identification of reaction conditions that enhance stereoselectivity, which was supported by computational studies that identified the solution-state catalyst structure. An evaluation of monomer substrates with systematic variations in steric parameters and functional group identities established key structure-reactivity relationships for stereoselective homo- and copolymerization. Expansion of the monomer scope to include enantioenriched vinyl ethers enabled the preparation of an isotactic poly(vinyl ether) with the highest stereoselectivity (95.1% ± 0.1 meso diads) reported to date, which occurred when monomer and catalyst stereochemistry were fully matched under a triple diastereocontrol model. The more complete understanding of stereoselective cationic polymerization reported herein offers a foundation for the design of improved catalytic systems and for the translation of isotactic poly(vinyl ether)s to applied areas.

#### INTRODUCTION

The stereochemistry of vinyl polymers has a profound effect on their material properties. As an illustrative example, atactic polypropylene is a viscoelastic fluid of little utility, whereas isotactic polypropylene (iPP) is a low-cost thermoplastic used in automotive, packaging, and structural applications at a volume exceeding 50 million metric tons annually.<sup>2</sup> Even though industrial iPP production is still dominated by heterogeneous catalysts, the discovery of homogeneous single-site transition metal catalysts for stereoselective  $\alpha$ -olefin polymerization has provided key mechanistic insight into the origin of stereocontrol.<sup>3-6</sup> This fundamental understanding has enabled the tailoring of catalyst coordination environment to precisely control polyolefin microstructure, leading to a dazzling array of thermomechanical properties from only a few  $\alpha$ -olefin building blocks. <sup>1,7,8</sup> Despite these impressive advances, a long-standing goal has been to incorporate polar functionality into polyolefins to enhance their interfacial properties.<sup>9,10</sup> An intrinsic challenge arises from the irreversible binding of Lewis basic heteroatoms with the electrophilic early transition metal catalysts traditionally used for stereoselective  $\alpha$ -olefin polymerization, which often precludes copolymerization with polar

monomers. 11 Late transition metal catalysts have been developed that succeed in copolymerizing polar vinyl monomers with ethylene, but their stereoselective copolymerization with  $\alpha$ -olefins is rare.  $^{7,9,12-19}$ 

The stereoselective homopolymerization of polar vinyl monomers is an attractive, but underdeveloped, approach to derive differentiated properties from underutilized yet readily available building blocks. One method that has demonstrated considerable success is stereoselective coordination-addition polymerization using electron-deficient single-site metal catalysts.<sup>20</sup> This mechanism proceeds through an eightmembered ring ester enolate chelate to stabilize the catalyst resting state, thereby limiting the scope of the polymerization to enolizable monomers. Steric interactions between the ligands, chain end, and monomer dictate stereoselective

Received: July 31, 2020 Published: September 28, 2020





monomer addition; thus, catalyst structure can require extensive optimization for each substrate of interest. <sup>21–25</sup>

Due to these limitations, the polymerization of polar vinyl monomers is typically conducted by radical or ionic mechanisms, where the propagating chain-end is a prochiral reactive intermediate with no obvious mode for biasing facial addition of monomer. Stereoselective polymerization, in the context of these methods, has traditionally been accomplished by chain-end control, whereby the stereochemistry of the last enchained monomer influences the facial addition of the next monomer (Figure 1A). 5,26–29 While this approach provides

# **A.** Previous work: Stereoselective polymerization via chain-end control

**B.** This work: Mechanistic studies of stereoselective polymerization via catalyst control

 Structure-reactivity relationships: R = linear, branched, functional, & enantioenriched substitution

$$= \underbrace{\begin{array}{c} A_{\Gamma} \\ O_{P} \\ O_{A_{\Gamma}} \end{array}}_{A_{\Gamma}} \underbrace{\begin{array}{c} A_{\Gamma} \\ O_{T} \\ O_{A_{T}} \end{array}}_{A_{\Gamma}} \underbrace{\begin{array}{c} A_{\Gamma} \\ A_{\Gamma} \\ O_{\Gamma} \\ O_{T} \end{array}}_{CF_{3}} \underbrace{\begin{array}{c} C_{\Gamma} \\ O_{T} \\ O_{T} \\ O_{T} \end{array}}_{CF_{3}} \underbrace{\begin{array}{c} C_{\Gamma} \\ O_{T} \\ O_{T} \\ O_{T} \\ O_{T} \end{array}}_{CF_{3}} \underbrace{\begin{array}{c} C_{\Gamma} \\ O_{T} \\$$

What governs stereoselectivity? Kinetic, stereoselectivity,
 & computational analyses uncover key energetic parameters

**Figure 1.** Approaches for the stereoselective polymerization of vinyl ether monomers.

stereoregular polymers in a number of cases, the level of stereoselectivity achieved is intrinsically linked to the steric demands of each individual substrate and therefore not broadly applicable, even within a monomer class.

Drawing inspiration from many biosynthetic pathways that involve asymmetric additions into oxocarbenium ions, <sup>30–34</sup> we recently reported a general approach for the stereoselective cationic polymerization of vinyl ethers (Figure 1B). In this system, stereoselectivity arises as a result of a chiral Lewis acid counterion derived from TiCl<sub>4</sub>(THF)<sub>2</sub> and a 3,3′-substituted-1,1′-bi-2-naphthol (BINOL)-based phosphoric acid.<sup>35</sup> Analysis of triad tacticity using Markovian statistics suggested an overwhelming preference for catalyst-controlled stereoselectivity, otherwise known as enantiomorphic site control.<sup>5,36–39</sup> In contrast to alternative methods for stereoselective vinyl ether polymerization, <sup>27,40–48</sup> our catalyst-controlled approach was broadly applicable to a variety of alkyl vinyl ether monomers, whose homopolymerization and copolymerization <sup>49</sup> resulted in diverse thermomechanical properties.

The expansion of the scope and utility of this method necessitated more comprehensive mechanistic investigations, similar to those that catalyzed the recent advancements in photocontrolled cationic polymerization. SO-56 As such, our

current mechanistic hypothesis is depicted in Figure 2. Addition of chiral BINOL-based phosphoric acid (R)-1 to a solution of TiCl<sub>4</sub> in toluene results in ligand exchange to generate a chiral Lewis acid (R)-2 concomitant with the release of HCl (Step I). Upon the addition of vinyl ether monomer to this reaction solution, the Markovnikov addition of HCl to the vinyl ether yields alkyl chloride 3, which was previously validated as an initiating species (Step II).35 Chloride abstraction from 3 generates an anionic titanium species (R)-4 along with oxocarbenium ion 5 (Step III), which serves as the active species for propagation. A low dielectric solvent facilitates a tight ion pair between (R)-4 and 5, enabling selective facial addition of each incoming monomer to the prochiral chain end (Step IV). Finally, chloride transfer from the anionic titanium species (R)-4 caps the polymer chain end and regenerates the active catalyst (Step V).

While our initial work established ion-pairing catalysis as a successful conceptual approach for stereoselective cationic polymerization, a deeper understanding of polymerization mechanism and catalyst identity is required to design improved systems and expand ion-pairing catalysis to a broader range of building blocks. Herein, we use a combination of kinetic investigations, temperature dependent stereoselectivity analyses, and computational studies to probe the elementary steps of the polymerization and to gain insight into catalyst solution structure. Collectively, the data reveals key criteria for stereoselectivity in vinyl ether polymerization and ultimately informs an expansion of the monomer scope of this method.

#### ■ RESULTS AND DISCUSSION

Kinetic Analysis of Stereoselective Vinyl Ether **Polymerization.** An analysis of vinyl ether polymerization kinetics identified key mechanistic insights that informed the selection of optimal stereoselective reaction conditions. Isobutyl vinyl ether (iBVE) was selected as a representative vinyl ether substrate for comparative analysis, and kinetic studies were conducted using in situ infrared (IR) spectroscopy to monitor the disappearance of the olefin signal at 1610 cm<sup>-</sup> throughout the course of the reaction. The stereoselective polymerization of iBVE using chiral Lewis acid (R)-2 ([iBVE] = 0.38 M, [(R)-1] = 5.0 mM,  $[TiCl_4]$  = 1.0 mM) was compared to a control polymerization catalyzed by achiral  $TiCl_4$  in the absence of Brønsted acid (R)-1. Our mechanistic hypothesis includes the endogenous formation of HCl and thus initiation of species 3 under the stereoselective polymerization conditions. Since this does not happen in the polymerization catalyzed by TiCl<sub>4</sub> alone, 3 was synthesized separately and added to the polymerization ([iBVE] = 0.38 M, [3] = 5.0 mM,  $[\text{TiCl}_4] = 1.0 \text{ mM}$ ). The Bovey formulizm is used to describe polymer tacticity, where meso diads (m) and racemo diads (r) are used to indicate enchainment that leads to isotactic diads and syndiotactic diads, respectively.

Initial rates of the two polymerizations displayed pseudo-first order reaction kinetics in both cases, consistent with previous observations for cationic polymerization. The rate constant of the conditions that resulted in stereoselective polymerization,  $k_{\rm obs} = 1.0 \times 10^{-3} \ {\rm s}^{-1}$ , was eight times slower than that of the control polymerization,  $k_{\rm obs} = 8.0 \times 10^{-3} \ {\rm s}^{-1}$  (Figure 3A). This significant decrease in rate observed with the addition of (R)-1 represents a case of ligand decelerated catalysis. The observed ligand deceleration fits with two notable previously reported empirical observations. First, the addition of TiCl<sub>4</sub> to a solution of iBVE and (R)-1 resulted in

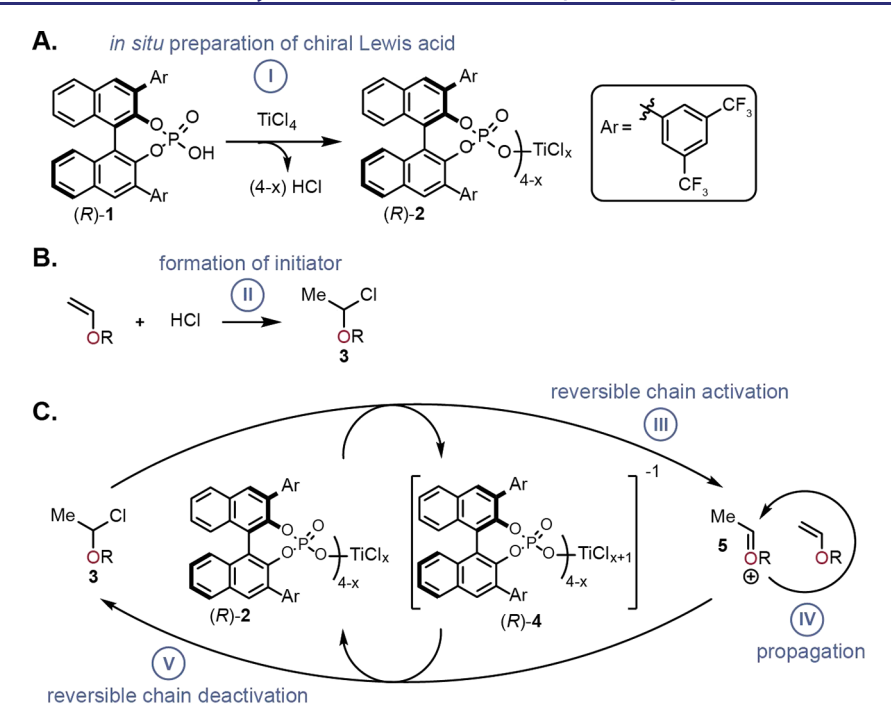


Figure 2. Proposed mechanism for the stereoselective polymerization of vinyl ethers.

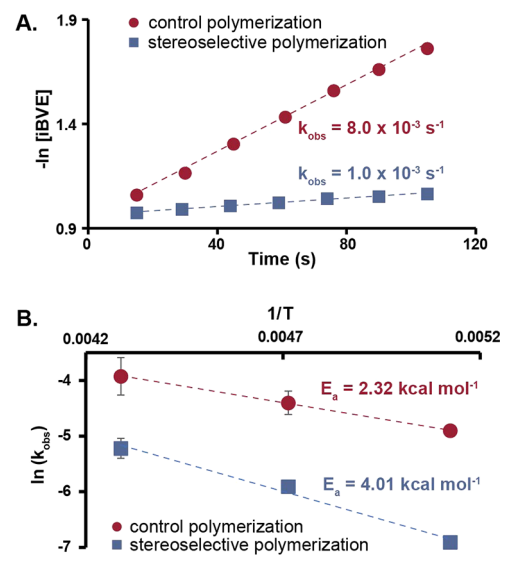


Figure 3. (A) Kinetic analysis of iBVE polymerization (2.25 mmol scale) at -78 °C under stereoselective conditions (blue squares; [iBVE] = 0.38 M, [(R)-1] = 5.0 mM, [TiCl<sub>4</sub>] = 1.0 mM) and control conditions (red circles; [iBVE] = 0.38 M, [3] = 5.0 mM, [TiCl<sub>4</sub>] = 1.0 mM). Data reported is the experimental data for the median  $k_{\rm obs}$  for each set of conditions. (B) Arrhenius analysis of stereoselective polymerization conditions (blue squares; [iBVE] = 0.38 M, [(R)-1] = 5.0 mM, [TiCl<sub>4</sub>] = 1.0 mM) and control polymerization conditions (red circles; [iBVE] = 0.38 M, [iBVE-Cl] = 5.0 mM, [TiCl<sub>4</sub>] = 1.0 mM) performed on a 2.25 mmol scale. Data reported at each temperature is the average of three individual polymerizations.

diminished stereoselectivity (82% m), compared to an analogous reaction where TiCl<sub>4</sub> and (R)-1 were premixed and iBVE was subsequently introduced (87% m). Second, the addition of excess ligand (R)-1 resulted in increased stereoselectivity, with at least five equivalents of (R)-1 compared to TiCl<sub>4</sub> required to obtain the highest selectivity. In both of these observations, the quantity of free TiCl<sub>4</sub> is minimized,

thus suppressing the faster, undesired nonstereoselective background reaction.

Quantitative comparisons of the energy required for monomer addition were obtained by monitoring the kinetics of polymerization by *in situ* IR at different temperatures. An Arrhenius plot of the natural log of  $k_{\rm obs}$  as a function of reciprocal temperature yielded a straight line and allowed the derivation of the activation energy  $(E_{\rm a})$  for polymerization (Figure 3B). A significant increase in  $E_{\rm a}$  was observed for the stereoselective polymerization  $(E_{\rm a}=4.01~{\rm kcal/mol})$  relative to the control reaction  $(E_{\rm a}=2.32~{\rm kcal/mol})$ . This quantitative data fits our hypothesis of ligand decelerated catalysis upon addition of (R)-1 to TiCl<sub>4</sub>. Additionally, the low values for  $E_{\rm a}$  in both polymerizations corroborate the rapid kinetics observed in cationic vinyl ether polymerization.

**Stereoselectivity Analysis.** Our previous optimization studies demonstrated a temperature effect on stereoselective polymerization, wherein lower temperatures resulted in enhanced stereoselectivity. In order to gain a quantitative understanding of the influence of temperature on stereoselectivity, an Eyring analysis was performed according to a modification of the Eyring eq (eq 1) by plotting the natural log of the ratio of *meso:racemo* diads vs the reciprocal temperature at which the polymerizations were conducted (Figure 4A)

$$\ln\left(\frac{\%m}{\%r}\right) = \frac{-\Delta\Delta H^{\ddagger}}{RT} + \frac{\Delta\Delta S^{\ddagger}}{R} \tag{1}$$

From the Eyring analysis, the difference in the energy between diastereomeric transition states ( $\Delta\Delta G^{\ddagger}$ ) can be extracted. We chose to use (R)-2 as the chiral Lewis acid for these studies, which achieves 87% m at -78 °C. While the use of a chiral Lewis acid derived from (R)-1 and  $\mathrm{TiCl_4(THF)_2}$  achieves higher tacticity (91% m at -78 °C), this system is more temperature sensitive and did not result in high molecular weight polymers over a broad temperature range, which made temperature dependent analysis impractical.

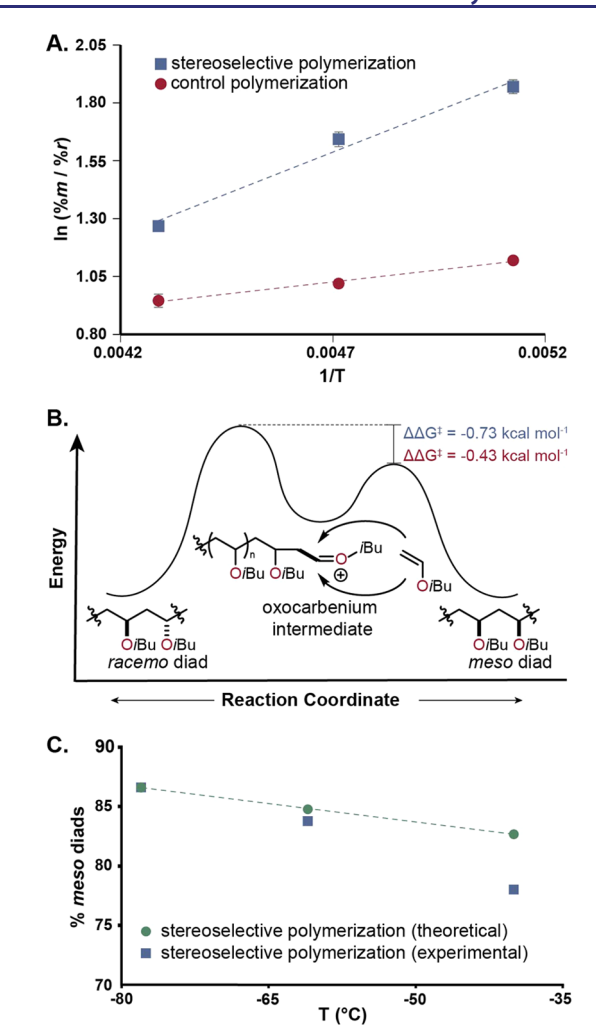


**Figure 4.** (A) Eyring analysis of both the stereoselective polymerization (blue squares; [iBVE] = 0.38 M, [(R)-1] = 5.0 mM,  $[TiCl_4] = 1.0 \text{ mM}$ ) and the control polymerization (red circles; [iBVE] = 0.38 M, [iBVE-Cl] = 5.0 mM,  $[TiCl_4] = 1.0 \text{ mM}$ ) performed on a 2.25 mmol scale. Each data point represents the average of three polymerizations. (B) Representative reaction coordinate diagram illustrating the greater energetic preference for *meso* diad formation during stereoselective polymerization. (C) Theoretical model of stereoselectivity assuming only two diastereomeric reaction pathways and experimental data demonstrating the deviation from theory via other less stereoselective pathways.

Polymerizations were not evaluated above  $-40\,^{\circ}\mathrm{C}$  because the reaction results in only oligomeric products, presumably due to a high degree of chain transfer events commonly observed in cationic polymerizations. <sup>69</sup>

The linear relationship observed for both the stereoselective and control polymerizations demonstrates that neither the overall mechanism nor the rate-determining step changes between -78 °C and -40 °C. The control polymerization catalyzed by TiCl<sub>4</sub> achieves 71% m at -78 °C, which results in a  $\Delta\Delta G^{\ddagger}$  of -0.43 kcal/mol; the significant stereoinduction is attributed to a chain-end control effect, which is commonly observed for Lewis acid catalyzed polymerizations of vinyl ethers. <sup>69,70</sup> The polymerization facilitated by chiral Lewis acid (R)-2 at -78 °C was found to have a  $\Delta\Delta G^{\ddagger}$  of -0.73 kcal/mol and a corresponding stereoselectivity of 87% m, confirming a preference toward meso diad formation. Therefore, addition of (R)-1 to TiCl<sub>4</sub> increases the kinetic barrier differentiating meso

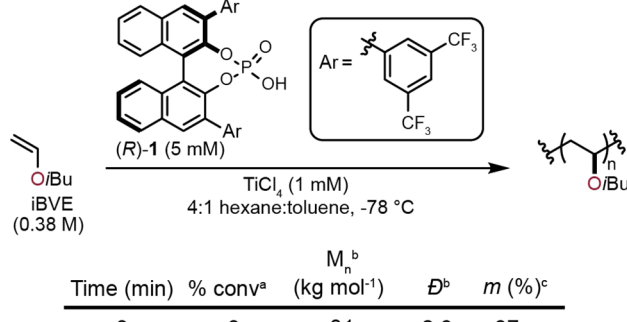
vs racemo addition by 0.30 kcal/mol, resulting in an increase of 16% m (Figure 4B).

Accurate determination of  $\Delta\Delta G^{\ddagger}$  in this context assumes that only two diastereomeric reaction pathways contribute to the outcome of the reaction (i.e., the addition of a monomer to the polymer chain end to achieve either a *meso* or *racemo* diad). To probe the magnitude of contributions from alternative reaction pathways, the experimental tacticity observed at -78 °C was used to calculate  $\Delta\Delta G^{\ddagger}$  according to eq 2. Using this energetic value, a theoretical % m vs temperature line was graphed assuming a purely two-state model

$$\Delta \Delta G^{\ddagger} = -RT \ln \left( \frac{\%m}{\%r} \right) \tag{2}$$

As shown in Figure 4C, the agreement between the experimental and theoretical data is strong at colder temperatures, indicating that a majority of monomer addition is influenced by chiral counterion (R)-4. As temperature increases, the deviation from theory grows, suggesting that an increasing portion of monomer addition is the result of a Ti species that is not the preferred catalyst. The contributions of these less-stereoselective catalytic pathways are presumably exaggerated due to the ligand-deceleration effect of (R)-1 (vide supra).

The small energetic difference that favors stereoselectivity and the known oxophilicity of titanium Lewis acid complexes motivated us to investigate whether dynamic nonlinear effects, resulting from catalyst—product or catalyst—substrate interactions, cause stereoselectivity to vary during the course of the polymerization. The experimental approach involved quenching aliquots of a polymerization at various time points and measuring reaction conversion and tacticity by  $^{1}$ H and  $^{13}$ C NMR, respectively. As shown in Figure 5, the tacticity remained constant at 87% m throughout the reaction, indicating that the growing isotactic poly(vinyl ether) (PVE) does not influence the ability of the catalyst to impart stereoselectivity. Furthermore, measurement of the molar mass  $(M_n)$  and dispersity (D) by gel permeation chromatography



Time (min)	% convª	(kg mol <sup>-1</sup> )	Ð♭	m (%)°
3	8	31	2.6	87
6	22	38	3.5	87
10	37	47	2.9	87
18	71	101	2.3	87

**Figure 5.** Monitoring the stereoselectivity of the polymerization as a function of conversion. Polymerizations performed on a 0.76 mmol scale. (a) Monomer conversion as determined by <sup>1</sup>H NMR integration relative to 1,4-dimethoxybenzene as an internal standard. (b) Number-average molecular weight and dispersity as characterized via GPC. (c) % *m* characterized via <sup>13</sup>C NMR integration.

(GPC) at the different time points demonstrated that this polymerization proceeds by an uncontrolled chain-growth mechanism with high molecular weights even at low conversion. We hypothesize this phenomenon is due to fast propagation compared to initiation.

Computational Analysis of Catalyst Structure. An understanding of the solution state structure of (R)-2 would inform the future optimization of stereoselective cationic polymerization methodology. In an initial attempt to probe the ligand sphere of (R)-2, we performed a series of iBVE polymerizations with varying ratios of (R)-1:TiCl<sub>4</sub> (Figure 6).

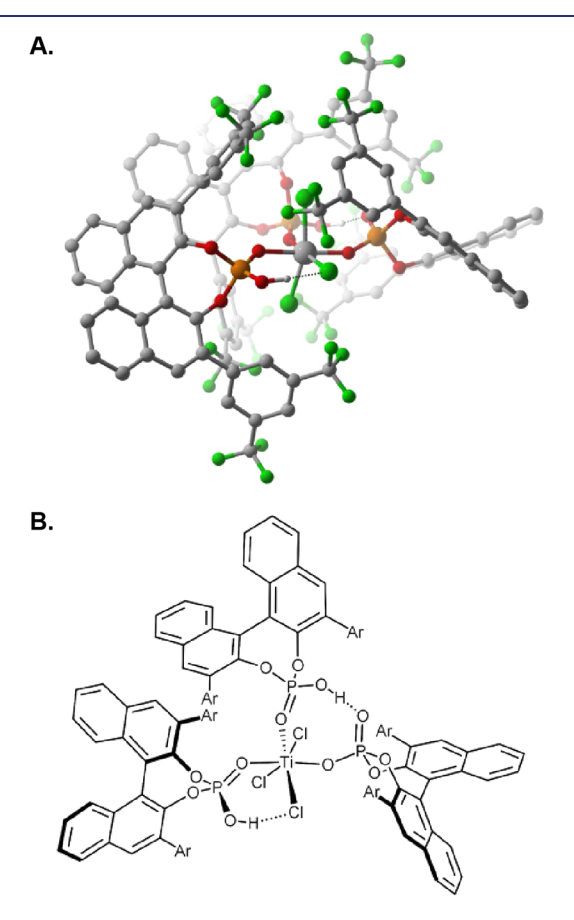
$$(R)-1 : TiCl_{4} \quad (MM) \quad (R)-1 \quad (MM) \quad ($$

Figure 6. Tacticity analysis of poly(iBVE) obtained using varying ratios of (R)-1:TiCl<sub>4</sub>. Polymerizations performed on a 0.76 mmol scale. (a) Number-average molecular weight and dispersity as characterized via GPC. (b) Percent *meso* diads as characterized via <sup>13</sup>C NMR integration.

A molar excess of (R)-1 relative to TiCl<sub>4</sub> was found to be required for effective stereoinduction during monomer addition. While equimolar amounts of (R)-1 and TiCl<sub>4</sub> resulted in poly(iBVE) with 76% m, an increase to 84% m was observed upon using a 2-fold excess of (R)-1 relative to TiCl<sub>4</sub>. Further increasing this ratio enabled the preparation of poly(iBVE) materials with increasing levels of isotacticity up to 87% m. This data, in combination with our previously reported experimental observations and <sup>31</sup>P NMR data,<sup>74</sup> contribute to a hypothesis where the complex responsible for the observed stereoselectivity is ligated by multiple phosphate ligands. In addition, the degree to which this desired complex exists in equilibrium is aided by superstoichiometric (R)-1 relative to TiCl<sub>4</sub>.

Given the dynamic nature of the proposed equilibrium process, it remains difficult to directly probe the solution-state structure of the chiral catalyst responsible for achieving highly isotactic PVEs. Indeed, attempts to crystallize any (R)-1-ligated Ti species were unsuccessful, and low-temperature NMR studies provided only qualitative observations of catalyst structure. Thus, we sought to utilize density functional theory (DFT) to investigate the structure computationally. Geometry optimizations using SMD(n-hexane)/MN15/6-311+G(d,p) def2-TZVP and SDD(Ti)//M06/def2-SVP, LANL2DZ(Ti) basis sets were performed on titanium tetrachloride in the presence of one, two, or three equivalents of (R)-1. A number of reasonable structures were found (see Figures S6–S8), and analysis of the relative free energies of these structures revealed the most optimal ligand geometry. The lowest energy

conformation computed was a conformer of  $TiCl_3((R)-1)_3$ , where one equivalent of HCl has been released, and the (R)-1 ligands all exist on the same plane of an overall octahedral geometry (Figure 7). This structure bearing multiple



**Figure 7.** (A) Three-dimensional ball and stick model of the lowest energy conformation of (R)-1 ligand interacting with TiCl<sub>4</sub>, upon release of 1 equiv of HCl. (B) Bond-line representation of the same complex.

phosphate ligands is consistent with our previous data whereby multiple equivalents of the (R)-1 ligand were necessary to achieve highly isotactic PVEs. Additionally, we previously hypothesized that HCl released upon (R)-1 ligation to  $\mathrm{TiCl_4}$  acts as an endogenous initiating species, again agreeing with this computationally derived structure.

Substrate Scope. An understanding of the scope of catalyst (R)-2 with a diversity of monomers connects kinetic and computational studies to the performance of the method. To compare substrates against one another under conditions that achieve high stereoselectivity, we conducted all polymerizations at −78 °C and used TiCl<sub>4</sub>(THF)<sub>2</sub> as a Lewis acid. The ratio of (R)-1 to TiCl<sub>4</sub>(THF)<sub>2</sub> was fixed at 5:1, and the reactions were conducted at a monomer concentration of 0.38 M on a 0.76 mmol scale. Initially, commercially available alkyl vinyl ether monomers with linear side chains were explored and found to be well-tolerated in the stereoselective polymerization. In addition to ethyl vinyl ether (EVE), n-propyl vinyl ether (nPrVE), and n-butyl vinyl ether (nBVE), which were previously shown to engender isotactic PVEs, 35 the polymerization of octyl vinyl ether (OcVE) also yielded an isotactic material (94% m). Despite the demonstration of a slightly higher level of isotacticity as chain length increased, a

corresponding decrease in the melting temperature  $(T_{\rm m})$  of the materials was observed (Figure 8A). This observation suggests that the conformational flexibility of the side chains has an impact on polymer crystallization within this series.<sup>75</sup>

**Figure 8.** Representative structure—property and structure—reactivity profiles for a variety of vinyl ethers. Polymers prepared using optimized reaction conditions ([iBVE] = 0.38 M, [(R)-1] = 5.0 mM, [TiCl<sub>4</sub>(THF)<sub>2</sub>] = 1.0 mM) at  $-78 \,^{\circ}\text{C}$  in 4:1 hexane/toluene on a 0.76 mmol scale.

The steric properties of branched alkyl vinyl ether monomers demonstrated a pronounced influence on the stereoselectivity achieved with catalyst (R)-2 (Figure 8B). In order to probe these effects systematically, the site of branching was placed progressively closer to the ether through the evaluation of isoamyl vinyl ether (iAVE), iBVE, and isopropyl vinyl ether (iPVE). While iAVE and iBVE demonstrated similar stereoselectivity (90 and 91% m, respectively), a decrease in isotacticity was observed when the branch point was placed  $\alpha$  to the vinyl ether in iPVE (88% m). Within this series, the  $T_{\rm m}$  of the isotactic PVEs increased as the branch point was placed progressively closer to the ether, indicating that compact side chains lead to higher melting isotactic PVEs. In contrast, the presence of a quaternary center  $\alpha$  to the vinyl ether, such as in *tert*-butyl vinyl ether (tBVE), proved to be detrimental to stereoselectivity, resulting in poly(tBVE) with 75% m and no discernible melting temperature. This systematic screen of monomer steric parameters implies that increasing steric hindrance close to the ether oxygen results in a diminished stereoselectivity during polymerization. Our proposed mechanism indicates that facial addition in these polymerizations is biased by the close association of the cationic chain-end with anionic counterion (R)-4 (Step IV in Figure 2). Therefore, we hypothesize that an increase in steric bulk close to the oxocarbenium ion disrupts the tight ion pair and causes a decrease in the stereoselectivity of monomer addition.<sup>76–78</sup>

The polymerization of vinyl ether substrates that contain polar functional groups would expand the potential utility of isotactic PVEs. To interrogate the functional group compatibility of catalyst (R)-2, we identified a series of vinyl ether monomers with functionality connected via an ethylene glycol spacer. This approach provided a systematic comparison of functional groups while they remained isoelectronic at the vinyl ether. Initial trials indicated that none of the monomers in Figure 9 underwent homopolymerization using catalyst (R)-2, presumably due to deleterious interactions of Lewis basic functionality on the substrates with the oxophilic Ti Lewis acid. The substrates with the oxophilic Ti Lewis acid.

Our previous demonstration of stereoselective copolymerization of vinyl ethers  $^{49}$  using catalyst (*R*)-2 inspired the exploration of functional group rich vinyl ethers as comonomers in the catalyst-controlled methodology. For these copolymers, iBVE was used as a representative alkyl vinyl ether comonomer and various substituted oxyethylene vinyl ethers (ROVE, where R is a variable substituent) were included at a specified molar fraction ( $f_{\rm ROVE}$ ) relative to iBVE. In the isolated copolymer, distinct  $^1H$  NMR resonances of iBVE and ROVE repeat units were integrated relative to each other in order to determine the actual molar incorporation of ROVE ( $F_{\rm ROVE}$ ).

We first investigated the functional comonomer 2-methoxy ethyl vinyl ether (MOVE), which has been shown to chelate with a growing cationic chain end and increase the rate of polymerization under Lewis acid catalyzed conditions. When  $f_{\text{MOVE}} = 0.20$  or below (Figure 9 entries 1–2, see SI for additional experiments), high monomer conversions (>73%) and isotactic copolymers (89–91% m) were observed, with  $F_{\text{MOVE}}$  remaining similar to  $f_{\text{MOVE}}$ . Attempts to achieve higher incorporations of MOVE by increasing  $f_{\text{MOVE}}$ , however, led to significant decreases in overall monomer conversion and tacticity (entries 3–4).

We next investigated phenoxy ethyl vinyl ether (PhOVE), which represents a phenyl ether functionality that is less Lewis basic than the alkyl ether in MOVE. A consistent increase in  $F_{PhOVE}$  was observed as  $f_{PhOVE}$  increased, albeit concomitant with a decrease in the overall monomer conversion (entries 5-9). Notably,  $F_{PhOVE}$  reached a maximum of 0.22 while retaining high isotacticity (90% m), demonstrating the promise of incorporating significant amounts of phenyl ether functionality into isotactic PVEs. Since phenyl ethers are prominent in numerous small molecule derivatives of lignin, 74,82–84 we chose to study a vinyl ether monomer derived from creosol as a representative lignin derivative. The vinyl ether monomer 2methoxy-4-methyl-phenoxy ethyl vinyl ether (MOPhOVE) was synthesized from creosol and subjected to the stereoselective polymerization conditions (entries 10–13). At  $f_{MOPhOVE} = 0.05$ , copolymerization proceeds to 50% conversion and yields a copolymer of  $F_{\text{MOPhOVE}}$  = 0.04 and 92% m. An interesting phenomenon was observed where increasing  $f_{\text{MOPhOVE}}$  has little influence on  $F_{\text{MOPhOVE}}$  or isotacticity. Overall, the phenyl ether substituents were tolerated better than the methyl ether groups and enabled the incorporation of the lignin derived MOPhOVE into isotactic PVE copolymers.

Carbonyl groups represent a functional group class with a rich array of accessible chemistry. Acetoxy ethyl vinyl ether (AcOVE) was investigated as the simplest ester-containing vinyl ether monomer for stereoselective polymerization. AcOVE demonstrated a pronounced poisoning effect on catalyst (R)-2. While addition of  $f_{AcOVE} = 0.01$  as a comonomer with iBVE resulted in a material with 2 mol % AcOVE while retaining high levels of isotacticity (92% m) and monomer

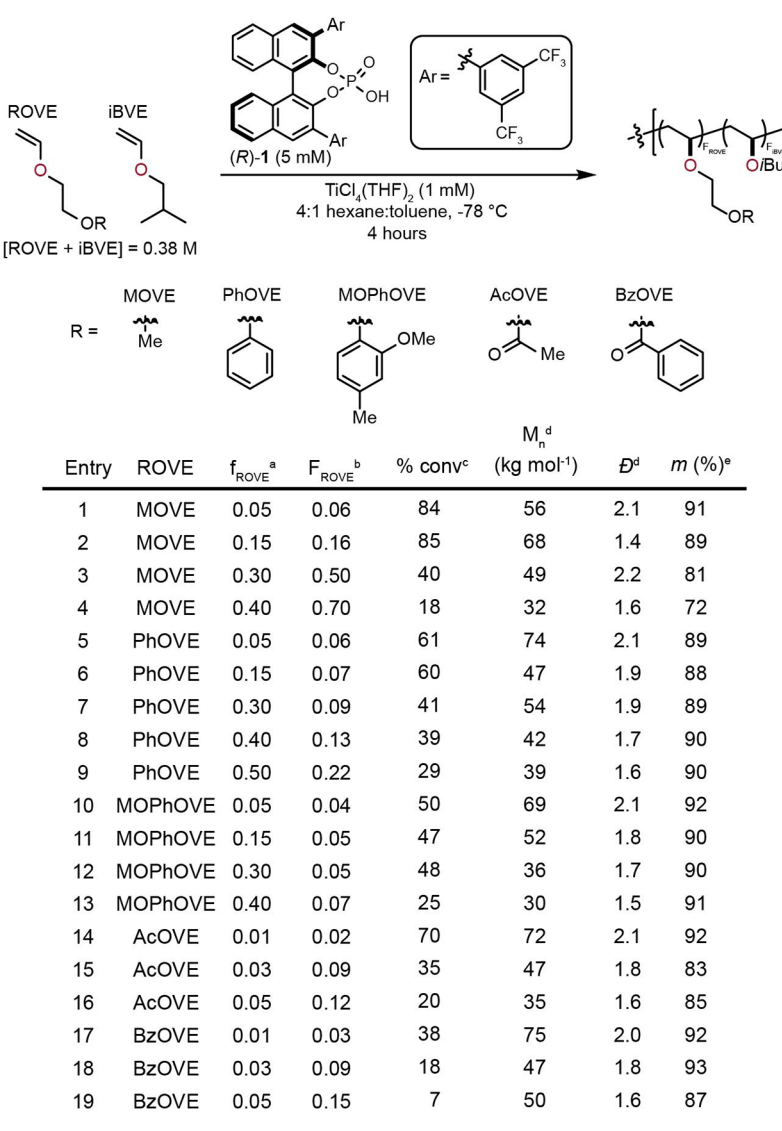


**Figure 9.** Structure—reactivity analysis of functional comonomers bearing Lewis basic sites. Polymerizations performed on a 1.0 mmol total vinyl ether monomer scale. (a) Molar fraction of the functional comonomer (ROVE) relative to iBVE in the initial reaction solution prior to initiation (i.e., f<sub>ROVE</sub> = 0.05 is 5 mol % ROVE and 95 mol % iBVE). (b) Mole fraction of ROVE in final copolymer as determined by <sup>1</sup>H NMR integration. (c) Monomer conversion as determined by <sup>1</sup>H NMR integration relative to 1,4-dimethoxybenzene as an internal standard. (d) Number-average molecular weight and dispersity as characterized via GPC. (e) Percent *meso* diads as characterized via <sup>13</sup>C NMR integration.

conversion (70%), the inclusion of higher concentrations of AcOVE had a negative effect on both overall monomer conversion and tacticity (entries 15-16). Benzoyloxy ethyl vinyl ether (BzOVE) represented an ester-containing monomer that performed better in the stereoselective copolymerization. The copolymerization of BzOVE and iBVE resulted in copolymers with moderate conversions (18-38%) and high isotacticities (92–93% m) with  $F_{BzOVE}$  values up to 0.09. BzOVE incorporation higher than 9 mol % decreased both conversion and tacticity (entry 19). Overall, the culmination of these experiments demonstrates that catalyst (R)-2 can successfully incorporate functional vinyl ether monomers through copolymerization. We observed that Lewis basic functionality in comonomers can reduce overall catalyst efficiency and stereoselectivity; however, this can be mitigated to an extent by incorporating phenyl groups that increase the steric environment and decrease the overall Lewis basicity of oxygen-rich vinyl ethers.

**Role of Chirality.** A key aspect of stereoselective vinyl ether polymerization by (R)-2 is that it proceeds by enantiomorphic site control,  $^{5,26}$  whereby a stereochemical error during monomer enchainment is corrected during subsequent monomer addition. This implies that the catalyst is primarily responsible for achieving facial discrimination during monomer enchainment, and it can override the influence of the stereochemistry of the last enchained monomer unit. While enantiomorphic site control is commonly observed in coordination—insertion polymerization approaches, it is rarely reported in ionic polymerizations;  $^{85-92}$  therefore, we endeavored to study this phenomenon in more depth.

We hypothesized that the axial chirality of the (R)-1 ligand serves an influential role in stereoselective polymerization. However, the difficulty understanding the exact catalyst solution structure and the dynamic nature of ligands on titanium complicate experimental design and analysis. In an attempt to initially explore the role of ligand chirality in our

system, we polymerized iBVE in our optimized reaction conditions with differing enantiomeric ratios of the phosphoric acid ligand 1 (see Figure S12), and in all cases, the tacticity of the resultant polymer was not affected. A similar phenomenon was recently observed by Aoshima and co-workers in the cationic polymerization of vinyl ethers using a titanium Lewis acid ligated with  $\alpha,\alpha,\alpha',\alpha'$ -tetraaryl-1,3-dioxolane-4,5- dimethanol (TADDOL),<sup>48</sup> wherein they hypothesized the initiating catalyst remains with the polymer chain-end throughout propagation. While this could presumably be occurring herein, the difficulty in understanding the exact catalyst solution structure and the dynamic nature of ligands on titanium complicated quantitative correlations. In response to these intriguing results, we sought out a complementary experimental approach to further probe the influence of ligand stereochemistry on reaction outcome.

We hypothesized that the absolute stereochemistry of the phosphoric acid ligands in catalyst 2 may play a role in the stereochemical outcome of polymerizations using monomers bearing pendant enantioenriched substitution through a match-mismatch effect. The polymerization of an enantioenriched monomer with a chiral catalyst to yield an isotactic polymer represents a case where a triple diastereoselection model may be operative. Each monomer enchainment event involves two chiral reactants (i.e., the attacking monomer and the chain end bearing a pendant stereocenter) and one chiral catalyst. While double diastereoselection has been probed in detail in small molecule asymmetric catalysis, 93,94 triple diastereoselection represents a case of match-mismatch catalysis that remains underexplored. 95-98 In cases of triple diastereoselection, the interaction of three stereocenters adds the possibility of a partially matched case, in addition to a fully matched and fully mismatched case.7

To probe potential match-mismatch effects in the stereoselective polymerization of vinyl ethers, we synthesized two substrates with stereogenic centers placed in differing proximity to the vinyl ether. The first monomer, (S)-2methylbutyl vinyl ether ((S)-MBVE), possesses a stereocenter  $\beta$  to the ether oxygen. A control polymerization initiated by triflic acid generated a polymer of 70% m (Figure 10). We reasoned that the noncoordinating triflate counteranion enabled the best assessment of the influence of monomer chirality on the resulting tacticity of the material, absent from counterion effects. This stereoselectivity is analogous to the polymerization of achiral iBVE under the same conditions (71% m), which demonstrates that the stereochemistry of this substrate plays no discernible role on the stereoselectivity of polymerization. (S)-MBVE was subsequently subjected to reaction conditions using either enantiomer of phosphoric acid 1. In the presence of catalyst (R)-2, a polymer with 89.6  $\pm$ 0.1% m is produced, while in the presence of catalyst (S)-2, a polymer with 92.5  $\pm$  0.5% m is produced. These levels of stereoselectivity are similar to those observed when using (R)-2 or (S)-2 in the polymerization of iBVE (91% m with either enantiomer of 1). Regarding (S)-MBVE, the lack of stereoselectivity without the presence of 1 and the high stereoselectivity achieved in the presence of either enantiomer of 1 indicates a preference for the reaction outcome to be dictated by the catalyst, which supports the enantiomorphic site control we observe using (R)-2 with achiral monomers. We hypothesize that these results represent fully matched (92.5  $\pm$  0.5% m) and partially matched (89.6  $\pm$  0.1% m) examples of stereoselective polymerization.

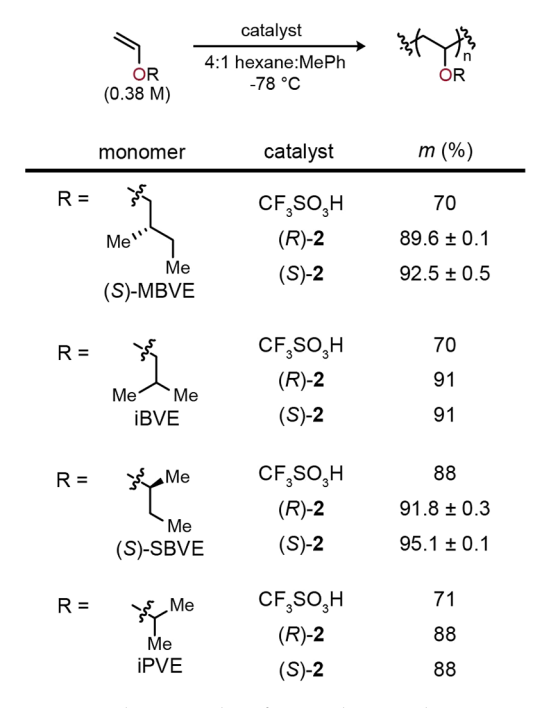


**Figure 10.** Match-mismatch effect analysis. Polymerizations performed on a 0.76 mmol scale. The polymerizations of the two chiral monomers with (R)-2 and (S)-2 were conducted three times, and standard deviation for m (%) were calculated from  $^{13}$ C NMR analysis of the three individual polymer samples.

In a complementary set of experiments, (S)-sec-butyl vinyl ether ((S)-SBVE) was synthesized to serve as a monomer with a stereocenter  $\alpha$  to the oxygen. Polymerization initiated by triflic acid resulted in a PVE with 88% m (Figure 10). Compared to the polymerization of achiral iPVE under identical conditions (71% m), a pronounced influence of substrate stereochemistry is observed. To probe the influence of catalyst stereochemistry on polymerization outcome, (S)-SBVE was subjected to the reaction conditions using either enantiomer of the chiral phosphoric acid (Figure 10). In the presence of catalyst (R)-2, a polymer with 91.8  $\pm$  0.3% m is produced while in the presence of catalyst (S)-2, a polymer with 95.1  $\pm$  0.1% m is produced. We hypothesize the use of (R)-2 results in a partially matched case. For the polymerization catalyzed by (S)-2, a fully matched system appears to be evident that enables both substrate and catalyst stereocontrol to contribute to the reaction outcome. These synergistic effects result in isotactic poly((S)-SBVE) at 95.1  $\pm$  0.1% m, which represents the highest stereoselectivity ever reported for a vinyl ether polymerization.

In the analysis of isotactic PVEs derived from enantioenriched monomers, the quantification of % m with standard deviations between 0.1 and 0.5 demonstrates the significance, accuracy, and reproducibility of both our synthetic methodology and  $^{13}\mathrm{C}$  NMR measurements. This difference in stereoselectivity is further highlighted when considering the thermal properties of these polymers. Differential scanning calorimetry (DSC) analysis at a scan rate of 10 °C/min with data taken from the second heating cycle revealed that poly((S)-MBVE) with 89.6  $\pm$  0.1% m shows a  $T_{\rm m}$  at 98 °C, while poly((S)-MBVE) with 92.5  $\pm$  0.5% m shows a  $T_{\rm m}$  at 104 °C (see Figures S58–S59). In poly((S)-SBVE), a more pronounced relationship between tacticity and thermal properties is observed. Poly((S)-SBVE) with 91.8  $\pm$  0.3% m lacks a

 $T_{\rm m}$ , while poly((S)-SBVE) with 95.1  $\pm$  0.1% m shows a  $T_{\rm m}$  at 137 °C (see Figures S63–S65). This suggests that achieving a fully matched system is required to enable this polymer to undergo reversible crystallization.

The results presented herein indicate that the placement of a stereocenter  $\alpha$  to the vinyl ether results in the substrate stereocontrol having a larger influence on reaction outcome than if the stereocenter is more remote from the reactive center. This structure—selectivity relationship is commonly observed in asymmetric transformations of small molecules that are governed by double diastereocontrol, providing support to our observations. While more remains to be discovered regarding the influence of ligand chirality on vinyl ether polymerizations, these results indicate that stereochemically matched catalyst—monomer interactions represent a viable approach to push the stereoselectivity of ionic polymerizations to unprecedented levels and discover differentiated material properties from readily available building blocks.

#### CONCLUSION

Comprehensive kinetic, experimental, and computational studies have provided valuable knowledge regarding the stereoselective cationic polymerization of vinyl ethers facilitated by catalyst 2. Comparative kinetic studies revealed the importance of ligand deceleration effects in the design of reaction conditions and catalysts to achieve highly stereoselective polymerizations. Evaluation of the temperature dependence on stereoselectivity showed that the preferred catalyst structure resulted in a 0.73 kcal/mol preference for meso diad formation at -78 °C compared to polymerization catalyzed by TiCl<sub>4</sub> alone, while at increased temperatures, the presence of alternative titanium complexes resulted in diminished isotacticity. A computational investigation of the solution-state structure of (R)-2 revealed the likely preferred catalyst structure that consists of three chiral phosphoric acids ligated to titanium, which was supported by experimental observations. An expansion of the substrate scope of stereoselective vinyl ether polymerization was enabled by probing monomers with systematic variations in steric parameters and functional group identities. Increasing the alkyl chain length for linear substituents resulted in increasing isotacticity and decreasing  $T_{\rm m}$  values, while increasing the steric bulk of branched alkyl substituents in proximity to the vinyl ether decreased isotacticity. The method was also found to be tolerant of aryl, ether, and ester functionality in stereoselective copolymerizations. Lastly, we demonstrated the synergistic relationship between monomer and catalyst stereochemistry through an analysis of match-mismatch effects operating under a triple diastereoselection model. Placement of the stereocenter  $\alpha$  to the vinyl ether resulted in the highest reported level of isotacticity in a poly(vinyl ether) to date  $(95.1 \pm 0.1\% m)$ . This comprehensive study enabled both a significantly deeper understanding of the stereoselective cationic polymerization of vinyl ethers and established a broader platform for accessing advanced polar polymeric materials. We envision that this work will inform future catalyst and materials design related to stereoselective polymerization.

### ASSOCIATED CONTENT

#### Supporting Information

The Supporting Information is available free of charge at https://pubs.acs.org/doi/10.1021/jacs.0c08254.

Syntheses, experimental details, characterization data, supplementary figures (PDF)

#### AUTHOR INFORMATION

#### **Corresponding Author**

Frank A. Leibfarth — Department of Chemistry, The University of North Carolina at Chapel Hill, Chapel Hill, North Carolina 27599, United States; orcid.org/0000-0001-7737-0331; Email: FrankL@email.unc.edu

#### **Authors**

Travis P. Varner — Department of Chemistry, The University of North Carolina at Chapel Hill, Chapel Hill, North Carolina 27599, United States

Aaron J. Teator — Department of Chemistry, The University of North Carolina at Chapel Hill, Chapel Hill, North Carolina 27599, United States; oorcid.org/0000-0003-4890-2487

**Yernaidu Reddi** — Department of Chemistry, University of Minnesota, Minneapolis, Minnesota 55455, United States; orcid.org/0000-0002-6743-9582

Paige E. Jacky — Department of Chemistry, The University of North Carolina at Chapel Hill, Chapel Hill, North Carolina 27599. United States

Christopher J. Cramer – Department of Chemistry, University of Minnesota, Minneapolis, Minnesota 55455, United States; orcid.org/0000-0001-5048-1859

Complete contact information is available at: https://pubs.acs.org/10.1021/jacs.0c08254

#### Notes

The authors declare the following competing financial interest(s): A.J.T. and F.A.L. are listed as inventors on a provisional patent application describing the stereoregular polymerization of vinyl ether monomers (62/719,240).

#### ACKNOWLEDGMENTS

The methodology development and kinetic studies were supported by the Young Investigator Program of the Army Research Office (W911NF-19-1-0115). The substrate scope and chirality studies were supported by the National Science Foundation under a CAREER award (CHE-1847362). Funding for the computational modeling portion of this project was provided by the Center for Sustainable Polymers, a National Science Foundation supported Center for Chemical Innovation (CHE-1901635). We thank Prof. Jeff Aubé for expertise regarding *in situ* IR instrumentation. We also thank Prof. Joseph Templeton, Prof. Kevin Frankowski, and Dr. Andreas Wierschen for thoughtful discussions. We thank the Minnesota Supercomputing Institute (MSI) for providing key computational resources.

#### REFERENCES

- (1) Worch, J. C.; Prydderch, H.; Jimaja, S.; Bexis, P.; Becker, M. L.; Dove, A. P. Stereochemical Enhancement of Polymer Properties. *Nat. Rev. Chem.* **2019**, *3*, 514–535.
- (2) Busico, V. Giulio Natta and the Development of Stereoselective Propene Polymerization. *Adv. Polym. Sci.* **2013**, 257, 37–58.
- (3) Brintzinger, H. H.; Fischer, D.; Mülhaupt, R.; Rieger, B.; Waymouth, R. M. Stereospecific Olefin Polymerization with Chiral Metallocene Catalysts. *Angew. Chem., Int. Ed. Engl.* **1995**, 34 (11), 1143–1170.

- (4) Resconi, L.; Cavallo, L.; Fait, A.; Piemontesi, F. Selectivity in Propene Polymerization with Metallocene Catalysts. *Chem. Rev.* **2000**, *100* (4), 1253–1346.
- (5) W. Coates, G. Precise Control of Polyolefin Stereochemistry Using Single-Site Metal Catalysts. *Chem. Rev.* **2000**, *100* (4), 1223–1252.
- (6) Tabba, H. D.; Hijji, Y. M.; Abu- Surrah, A. S. Polyolefin Compounds and Materials: Fundamentals and Industrial Applications; Al-Ali AlMa'adeed, M., Krupa, I., Eds.; Springer International Publishing: Switzerland, 2016.
- (7) Domski, G. J.; Rose, J. M.; Coates, G. W.; Bolig, A. D.; Brookhart, M. Living Alkene Polymerization: New Methods for the Precision Synthesis of Polyolefins. *Prog. Polym. Sci.* **2007**, *32*, 30–92.
- (8) De Rosa, C.; Auriemma, F.; Di Capua, A.; Resconi, L.; Guidotti, S.; Camurati, I.; E. Nifant'ev, I.; P. Laishevtsev, I. Structure—Property Correlations in Polypropylene from Metallocene Catalysts: Stereodefective, Regioregular Isotactic Polypropylene. *J. Am. Chem. Soc.* **2004**, *126* (51), 17040—17049.
- (9) Franssen, N. M. G.; Reek, J. N. H.; de Bruin, B. Synthesis of Functional 'Polyolefins': State of the Art and Remaining Challenges. *Chem. Soc. Rev.* **2013**, 42 (13), 5809–5832.
- (10) Keyes, A.; Basbug Alhan, H. E.; Ordonez, E.; Ha, U.; Beezer, D. B.; Dau, H.; Liu, Y. S.; Tsogtgerel, E.; Jones, G. R.; Harth, E. Olefins and Vinyl Polar Monomers: Bridging the Gap for Next Generation Materials. *Angew. Chem., Int. Ed.* **2019**, *58* (36), 12370–12391.
- (11) Chen, J.; Gao, Y.; Marks, T. J. Early Transition Metal Catalysis for Olefin-Polar Monomer Copolymerization. *Angew. Chem.* **2020**, 59, 2–12.
- (12) Tan, C.; Chen, C. Emerging Palladium and Nickel Catalysts for Copolymerization of Olefins with Polar Monomers. *Angew. Chem., Int. Ed.* **2019**, 58 (22), 7192–7200.
- (13) Ito, S.; Nozaki, K. Coordination-Insertion Copolymerization of Polar Vinyl Monomers by Palladium Catalysts. *Chem. Rec.* **2010**, *10* (5), 315–325.
- (14) Boffa, L. S.; Novak, B. M. Copolymerization of Polar Monomers with Olefins Using Transition-Metal Complexes. *Chem. Rev.* **2000**, *100* (4), 1479–1494.
- (15) Zhang, W.; Waddell, P. M.; Tiedemann, M. A.; Padilla, C. E.; Mei, J.; Chen, L.; Carrow, B. P. Electron-Rich Metal Cations Enable Synthesis of High Molecular Weight, Linear Functional Polyethylenes. *J. Am. Chem. Soc.* **2018**, *140* (28), 8841–8850.
- (16) Nakamura, A.; Anselment, T. M. J.; Claverie, J.; Goodall, B.; Jordan, R. F.; Mecking, S.; Rieger, B.; Sen, A.; van Leeuwen, P. W. N. M.; Nozaki, K. Ortho-Phosphinobenzenesulfonate: A Superb Ligand for Palladium-Catalyzed Coordination—Insertion Copolymerization of Polar Vinyl Monomers. *Acc. Chem. Res.* **2013**, *46* (7), 1438–1449.
- (17) Carrow, B. P.; Nozaki, K. Transition-Metal-Catalyzed Functional Polyolefin Synthesis: Effecting Control through Chelating Ancillary Ligand Design and Mechanistic Insights. *Macromolecules* **2014**, *47* (8), 2541–2555.
- (18) Nakamura, A.; Ito, S.; Nozaki, K. Coordination–Insertion Copolymerization of Fundamental Polar Monomers. *Chem. Rev.* **2009**, *109* (11), 5215–5244.
- (19) Ittel, S. D.; Johnson, L. K.; Brookhart, M. Late-Metal Catalysts for Ethylene Homo- and Copolymerization. *Chem. Rev.* **2000**, *100* (4), 1169–1204.
- (20) Chen, E. Y.-X. Coordination Polymerization of Polar Vinyl Monomers by Single-Site Metal Catalysts. *Chem. Rev.* **2009**, *109* (11), 5157–5214.
- (21) Mariott, W. R.; Chen, E. Y.-X. Mechanism and Scope of Stereospecific, Coordinative-Anionic Polymerization of Acrylamides by Chiral Zirconocenium Ester and Amide Enolates. *Macromolecules* **2005**, 38 (16), 6822–6832.
- (22) Caporaso, L.; Cavallo, L. Mechanism of Stereocontrol in Methyl Methacrylate Polymerization Promoted by C1-Symmetric Metallocenes. *Macromolecules* **2008**, *41* (10), 3439–3445.
- (23) Zhang, Y.; Ning, Y.; Caporaso, L.; Cavallo, L.; Chen, E. Y.-X. Catalyst-Site-Controlled Coordination Polymerization of Polar Vinyl

- Monomers to Highly Syndiotactic Polymers. J. Am. Chem. Soc. 2010, 132 (8), 2695–2709.
- (24) Chen, X.; Caporaso, L.; Cavallo, L.; Chen, E. Y.-X. Stereoselectivity in Metallocene-Catalyzed Coordination Polymerization of Renewable Methylene Butyrolactones: From Stereo-Random to Stereo-Perfect Polymers. J. Am. Chem. Soc. 2012, 134 (17), 7278–7281.
- (25) Hu, Y.; Wang, X.; Chen, Y.; Caporaso, L.; Cavallo, L.; Chen, E. Y.-X. Rare-Earth Half-Sandwich Dialkyl and Homoleptic Trialkyl Complexes for Rapid and Stereoselective Polymerization of a Conjugated Polar Olefin. *Organometallics* **2013**, 32 (5), 1459–1465.
- (26) Okamoto, Y.; Nakano, T. Asymmetric Polymerization. *Chem. Rev.* **1994**, *94* (2), 349–372.
- (27) Ouchi, M.; Kamigaito, M.; Sawamoto, M. Stereoregulation in Cationic Polymerization by Designed Lewis Acids. II. Effects of Alkyl Vinyl Ether Structure. *J. Polym. Sci., Part A: Polym. Chem.* **2001**, 39 (7), 1060–1066.
- (28) Nomura, N.; Ishii, R.; Akakura, M.; Aoi, K. Stereoselective Ring-Opening Polymerization of Racemic Lactide Using Aluminum-Achiral Ligand Complexes: Exploration of a Chain-End Control Mechanism. J. Am. Chem. Soc. 2002, 124 (21), 5938–5939.
- (29) Weger, M.; Pahl, P.; Schmidt, F.; Soller, B. S.; Altmann, P. J.; Pöthig, A.; Gemmecker, G.; Eisenreich, W.; Rieger, B. Isospecific Group-Transfer Polymerization of Diethyl Vinylphosphonate and Multidimensional NMR Analysis of the Polymer Microstructure. *Macromolecules* **2019**, *52* (18), 7073–7080.
- (30) Sabini, E.; Sulzenbacher, G.; Dauter, M.; Dauter, Z.; Jørgensen, P. L.; Schulein, M.; Dupont, C.; Davies, G. J; Wilson, K. S Catalysis and Specificity in Enzymatic Glycoside Hydrolysis: A 2,5B Conformation for the Glycosyl-Enzyme Intermediate Revealed by the Structure of the Bacillus Agaradhaerens Family 11 Xylanase. *Chem. Biol.* 1999, 6 (7), 483–492.
- (31) Unrau, P. J.; Bartel, D. P. An Oxocarbenium-Ion Intermediate of a Ribozyme Reaction Indicated by Kinetic Isotope Effects. *Proc. Natl. Acad. Sci. U. S. A.* **2003**, *100* (26), 15393–15397.
- (32) Crich, D. Mechanism of a Chemical Glycosylation Reaction. Acc. Chem. Res. 2010, 43 (8), 1144–1153.
- (33) Gomez, H.; Polyak, I.; Thiel, W.; Lluch, J. M.; Masgrau, L. Retaining Glycosyltransferase Mechanism Studied by QM/MM Methods: Lipopolysaccharyl- $\alpha$ -1,4-Galactosyltransferase C Transfers  $\alpha$ -Galactose via an Oxocarbenium Ion-like Transition State. *J. Am. Chem. Soc.* **2012**, *134* (10), 4743–4752.
- (34) Adero, P. O.; Amarasekara, H.; Wen, P.; Bohé, L.; Crich, D. The Experimental Evidence in Support of Glycosylation Mechanisms at the SN1–SN2 Interface. *Chem. Rev.* **2018**, *118* (17), 8242–8284.
- (35) Teator, A. J.; Leibfarth, F. A. Catalyst-Controlled Stereoselective Cationic Polymerization of Vinyl Ethers. *Science* **2019**, *363*, 1439–1443.
- (36) Bovey, F. A.; Tiers, G. V. D. Polymer NSR Spectroscopy. II. The High Resolution Spectra of Methyl Methacrylate Polymers Prepared with Free Radical and Anionic Initiators. *J. Polym. Sci.* **1960**, 44 (143), 173–182.
- (37) Fueno, T.; Shelden, R. A.; Furukawa, J. Probabilistic Considerations of the Tacticity of Optically Active Polymers. J. Polym. Sci., Part A: Gen. Pap. 1965, 3, 1279–1288.
- (38) Doi, Y.; Asakura, T. Catalytic Regulation for Isotactic Orientation in Propylene Polymerization with Ziegler-Natta Catalyst. *Makromol. Chem.* **1975**, *176* (2), 507–509.
- (39) Byers, J. A.; Bercaw, J. E. Kinetic Resolution of Racemic  $\alpha$ -Olefins with Ansa-Zirconocene Polymerization Catalysts: Enantiomorphic Site vs. Chain End Control. *Proc. Natl. Acad. Sci. U. S. A.* **2006**, *103* (42), 15303–15308.
- (40) Fishbein, L.; Crowe, B. F. The Relation of Structure to Some Physical and Mechanical Properties of Poly(Vinyl Alkyl Ethers). *Makromol. Chem.* **1961**, 48 (1), 221–228.
- (41) Schildknecht, C. E.; Lee, C. H.; Long, K. P.; Rinehart, L. C. Some Aspects of Polymer Morphology: Time Dependence in Moephology of Polyvinyl Ethers and Polypropylenes. *Polym. Eng. Sci.* 1967, 7 (4), 257–263.

- (42) Natta, G.; Allegra, G.; Bassi, I. W.; Carlini, C.; Chiellini, E.; Montagnoli, G. Isomorphism Phenomena in Isotactic Poly (4-Methyl-Substituted  $\alpha$ -Olefins) and in Isotactic Poly(Alkyl Vinyl Ethers). *Macromolecules* **1969**, 2 (4), 311–315.
- (43) Aoshima, S.; Ito, Y.; Kobayashi, E. Stereoregularity of Poly(Vinyl Ether)s with a Narrow Molecular Weight Distribution Obtained by the Living Cationic Polymerization. *Polym. J.* **1993**, *25*, 1161–1168.
- (44) Ouchi, M.; Kamigaito, M.; Sawamoto, M. Stereoregulation in Cationic Polymerization by Designed Lewis Acids. 1. Highly Isotactic Poly(Isobutyl Vinyl Ether) with Titanium-Based Lewis Acids. *Macromolecules* **1999**, 32 (20), 6407–6411.
- (45) Ouchi, M.; Sueoka, M.; Kamigaito, M.; Sawamoto, M. Stereoregulation in Cationic Polymerization. III. High Isospecificity with the Bulky Phosphoric Acid [(RO)<sub>2</sub>PO<sub>2</sub>H]/SnCl<sub>4</sub> Initiating Systems: Design of Counteranions via Initiators. *J. Polym. Sci., Part A: Polym. Chem.* **2001**, 39 (7), 1067–1074.
- (46) Ohgi, H.; Sato, T. Highly Isotactic Poly(Vinyl Alcohol). III: Heterogeneous Cationic Polymerization of Tert-Butyl Vinyl Ether. *Polymer* **2002**, *43* (13), 3829–3836.
- (47) Kawaguchi, T.; Sanda, F.; Masuda, T. Polymerization of Vinyl Ethers with Transition-Metal Catalysts: An Examination of the Stereoregularity of the Formed Polymers. J. Polym. Sci., Part A: Polym. Chem. 2002, 40 (22), 3938–3943.
- (48) Watanabe, H.; Yamamoto, T.; Kanazawa, A.; Aoshima, S. Stereoselective Cationic Polymerization of Vinyl Ethers by Easily and Finely Tunable Titanium Complexes Prepared from Tartrate-Derived Diols: Isospecific Polymerization and Recognition of Chiral Side Chains. *Polym. Chem.* **2020**, *11*, 3398–3403.
- (49) Teator, A. J.; Varner, T. P.; Jacky, P. E.; Sheyko, K. A.; Leibfarth, F. A. Polar Thermoplastics with Tunable Physical Properties Enabled by the Stereoselective Copolymerization of Vinyl Ethers. ACS Macro Lett. 2019, 8 (12), 1559–1563.
- (50) Kottisch, V.; Michaudel, Q.; Fors, B. P. Cationic Polymerization of Vinyl Ethers Controlled by Visible Light. *J. Am. Chem. Soc.* **2016**, *138* (48), 15535–15538.
- (51) Michaudel, Q.; Kottisch, V.; Fors, B. P. Cationic Polymerization: From Photoinitiation to Photocontrol. *Angew. Chem., Int. Ed.* **2017**, *56* (33), 9670–9679.
- (52) Kottisch, V.; Michaudel, Q.; Fors, B. P. Photocontrolled Interconversion of Cationic and Radical Polymerizations. *J. Am. Chem. Soc.* **2017**, *139* (31), 10665–10668.
- (53) Michaudel, Q.; Chauvire, T.; Kottisch, V.; Supej, M. J.; Stawiasz, K. J.; Shen, L.; Zipfel, W. R.; Abruna, H. D.; Freed, J. H.; Fors, B. P. Mechanistic Insight into the Photocontrolled Cationic Polymerization of Vinyl Ethers. J. Am. Chem. Soc. 2017, 139 (43), 15530–15538.
- (54) Kottisch, V.; Supej, M. J.; Fors, B. P. Enhancing Temporal Control and Enabling Chain-End Modification in Photoregulated Cationic Polymerizations by Using Iridium-Based Catalysts. *Angew. Chem., Int. Ed.* **2018**, *57* (27), 8260–8264.
- (55) Peterson, B. M.; Kottisch, V.; Supej, M. J.; Fors, B. P. On Demand Switching of Polymerization Mechanism and Monomer Selectivity with Orthogonal Stimuli. *ACS Cent. Sci.* **2018**, *4* (9), 1228–1234.
- (56) Supej, M. J.; Peterson, B. M.; Fors, B. P. Dual Stimuli Switching: Interconverting Cationic and Radical Polymerizations with Electricity and Light. *Chem.* **2020**, *6* (7), 1794–1803.
- (57) Kojima, K.; Sawamoto, M.; Higashimura, T. Living Cationic Polymerization of Isobutyl Vinyl Ether by Hydrogen Iodide/Lewis Acid Initiating Systems: Effects of Lewis Acid Activators and Polymerization Kinetics. *Macromolecules* 1989, 22 (4), 1552–1557.
- (58) Cho, C. G.; Feit, B. A.; Webster, O. W. Cationic Polymerization of Isobutyl Vinyl Ether: Livingness Enhancement by Dialkyl Sulfides. *Macromolecules* **1990**, 23 (7), 1918–1923.
- (59) Hadjikyriacou, S.; Faust, R. Living Cationic Homopolymerization of Isobutyl Vinyl Ether and Sequential Block Copolymerization of Isobutylene with Isobutyl Vinyl Ether. Synthesis and Mechanistic Studies. *Macromolecules* **1995**, 28 (23), 7893–7900.

- (60) Sharpless, K. B. Coelacanths and Catalysis. *Tetrahedron* **1994**, 50 (15), 4235–4258.
- (61) Evans, D. A.; Murry, J. A.; Von, P. M.; Norcross, R. D.; Miller, S. J.; A Evans, I. D.; Murry, J. A.; von Matt, P.; Norcross, R. D.; Miller, S. J. C2-Symmetric Cationic Copper(II) Complexes as Chiral Lewis Acids: Counterion Effects in the Enantioselective Diels—Alder Reaction. *Angew. Chem., Int. Ed. Engl.* 1995, 34, 798–800.
- (62) Berrisford, D. J.; Bolm, C.; Sharpless, K. B. Ligand-Accelerated Catalysis. *Angew. Chem., Int. Ed. Engl.* 1995, 34, 1059–1070.
- (63) Evans, D. A.; Barnes, D. M.; Johnson, J. S.; Lectka, T.; von Matt, P.; Miller, S. J.; Murry, J. A.; Norcross, R. D.; Shaughnessy, E. A.; Campos, K. R. Bis(Oxazoline) and Bis(Oxazolinyl)Pyridine Copper Complexes as Enantioselective Diels—Alder Catalysts: Reaction Scope and Synthetic Applications. *J. Am. Chem. Soc.* 1999, 121 (33), 7582–7594.
- (64) Evans, D. A.; Burgey, C. S.; Kozlowski, M. C.; Tregay, S. W. C2-Symmetric Copper(II) Complexes as Chiral Lewis Acids. Scope and Mechanism of the Catalytic Enantioselective Aldol Additions of Enolsilanes to Pyruvate Esters. *J. Am. Chem. Soc.* **1999**, *121* (4), 686–699.
- (65) Ouchi, M.; Sueoka, M.; Kamigaito, M.; Sawamoto, M. Stereoregulation in Cationic Polymerization. III. High Isospecificity with the Bulky Phosphoric Acid [(RO)2PO2H]/SnCl4 Initiating Systems: Design of Counteranions via Initiators. *J. Polym. Sci., Part A: Polym. Chem.* **2001**, 39 (7), 1067–1074.
- (66) Knowles, R. R.; Lin, S.; Jacobsen, E. N. Enantioselective Thiourea-Catalyzed Cationic Polycyclizations. *J. Am. Chem. Soc.* **2010**, 132 (14), 5030–5032.
- (67) Ford, D. D.; Lehnherr, D.; Kennedy, C. R.; Jacobsen, E. N. Anion-Abstraction Catalysis: The Cooperative Mechanism of  $\alpha$ -Chloroether Activation by Dual Hydrogen-Bond Donors. *ACS Catal.* **2016**, *6* (7), 4616–4620.
- (68) Wang, X.-Y.; Sun, X.-L.; Wang, F.; Tang, Y. SaBOX/Copper Catalysts for Highly Syndio-Specific Atom Transfer Radical Polymerization of Methyl Methacrylate. ACS Catal. 2017, 7 (7), 4692–4696.
- (69) Kanazawa, A.; Kanaoka, S.; Aoshima, S. Major Progress in Catalysts for Living Cationic Polymerization of Isobutyl Vinyl Ether: Effectiveness of a Variety of Conventional Metal Halides. *Macromolecules* **2009**, 42 (12), 3965–3972.
- (70) Aoshima, S.; Kanaoka, S. A Renaissance in Living Cationic Polymerization. *Chem. Rev.* **2009**, *109* (11), 5245–5287.
- (71) Annamalai, V.; DiMauro, E. F.; Carroll, P. J.; Kozlowski, M. C. Catalysis of the Michael Addition Reaction by Late Transition Metal Complexes of BINOL-Derived Salens. *J. Org. Chem.* **2003**, *68* (5), 1973–1981.
- (72) Walsh, P. L.; C. Kozlowski, M. Fundamentals of Asymmetric Catalysis; University Science Books: Sausalito, CA, 2009.
- (73) Bryliakov, K. P. Dynamic Nonlinear Effects in Asymmetric Catalysis. ACS Catal. 2019, 9 (6), 5418-5438.
- (74) Shuai, L.; Amiri, M. T.; Questell-Santiago, Y. M.; Héroguel, F.; Li, Y.; Kim, H.; Meilan, R.; Chapple, C.; Ralph, J.; Luterbacher, J. S. Formaldehyde Stabilization Facilitates Lignin Monomer Production during Biomass Depolymerization. *Science* **2016**, *354* (6310), 329–333.
- (75) Trafara, G. State of Order in Isotactic Polyhexylethylene. J. Polym. Sci., Polym. Chem. Ed. 1980, 18 (1), 321–326.
- (76) Knowles, R. R.; Jacobsen, E. N. Attractive Noncovalent Interactions in Asymmetric Catalysis: Links between Enzymes and Small Molecule Catalysts. *Proc. Natl. Acad. Sci. U. S. A.* **2010**, *107* (48), 20678–20685.
- (77) Brak, K.; Jacobsen, E. N. Asymmetric Ion-Pairing Catalysis. *Angew. Chem., Int. Ed.* **2013**, 52 (2), 534–561.
- (78) Yepes, D.; Neese, F.; List, B.; Bistoni, G. Unveiling the Delicate Balance of Steric and Dispersion Interactions in Organocatalysis Using High-Level Computational Methods. *J. Am. Chem. Soc.* **2020**, 142 (7), 3613–3625.
- (79) Oda, Y.; Tsujino, T.; Kanaoka, S.; Aoshima, S. Lewis Acid-Specific Polymerization Behaviors in Living Cationic Polymerization

- of Vinyl Ether with a Malonate Group. J. Polym. Sci., Part A: Polym. Chem. 2012, 50 (15), 2993–2998.
- (80) Higashimura, T.; Aoshima, S.; Sawamoto, M. Vinyl Ethers with a Functional Group: Living Cationic Polymerization and Synthesis of Monodisperse Polymers. *Makromol. Chem., Macromol. Symp.* **1986**, 3 (1), 99–111.
- (81) Nakamura, T.; Aoshima, S.; Higashimura, T. Living Cationic Polymerization of Vinyl Ethers with a Functional Group. *Polym. Bull.* **1985**, *14* (6), 515–521.
- (82) O'Dea, R. M.; Willie, J. A.; Epps, T. H. 100th Anniversary of Macromolecular Science Viewpoint: Polymers from Lignocellulosic Biomass. Current Challenges and Future Opportunities. *ACS Macro Lett.* **2020**, *9*, 476–493.
- (83) Gandini, A. The Irruption of Polymers from Renewable Resources on the Scene of Macromolecular Science and Technology. *Green Chem.* **2011**, *13*, 1061–1083.
- (84) Zakzeski, J.; Bruijnincx, P. C. A.; Jongerius, A. L.; Weckhuysen, B. M. The Catalytic Valorization of Lignin for the Production of Renewable Chemicals. *Chem. Rev.* **2010**, *110* (6), 3552–3599.
- (85) Svirkin, Y. Y.; Xu, J.; Gross, R. A.; Kaplan, D. L.; Swift, G. Enzyme-Catalyzed Stereoelective Ring-Opening Polymerization of α-Methyl-β-Propiolactone. *Macromolecules* **1996**, 29 (13), 4591–4597.
- (86) Collins, S.; Ward, D. G.; Suddaby, K. H. Group-Transfer Polymerization Using Metallocene Catalysts: Propagation Mechanisms and Control of Polymer Stereochemistry. *Macromolecules* **1994**, 27 (24), 7222–7224.
- (87) Chisholm, M. H.; Patmore, N. J.; Zhou, Z. Concerning the Relative Importance of Enantiomorphic Site vs. Chain End Control in the Stereoselective Polymerization of Lactides: Reactions of (R,R-Salen)- and (S,S-Salen)-Aluminium Alkoxides LAIOCH2R Complexes (R = CH3 and S-CHMeCl). *Chem. Commun.* **2005**, No. 1, 127–129.
- (88) Darensbourg, D. J.; Karroonnirun, O.; Wilson, S. J. Ring-Opening Polymerization of Cyclic Esters and Trimethylene Carbonate Catalyzed by Aluminum Half-Salen Complexes. *Inorg. Chem.* **2011**, *50* (14), *6775–6787*.
- (89) Aluthge, D. C.; Patrick, B. O.; Mehrkhodavandi, P. A Highly Active and Site Selective Indium Catalyst for Lactide Polymerization. *Chem. Commun.* **2013**, 49 (39), 4295–4297.
- (90) Pilone, A.; Press, K.; Goldberg, I.; Kol, M.; Mazzeo, M.; Lamberti, M. Gradient Isotactic Multiblock Polylactides from Aluminum Complexes of Chiral Salalen Ligands. *J. Am. Chem. Soc.* **2014**, *136* (8), 2940–2943.
- (91) Altenbuchner, P. T.; Adams, F.; Kronast, A.; Herdtweck, E.; Pöthig, A.; Rieger, B. Stereospecific Catalytic Precision Polymerization of 2-Vinylpyridine via Rare Earth Metal-Mediated Group Transfer Polymerization with 2-Methoxyethylamino-Bis(Phenolate)-Yttrium Complexes. *Polym. Chem.* **2015**, *6* (38), 6796–6801.
- (92) Kronast, A.; Reiter, D.; Altenbuchner, P. T.; Vagin, S. I.; Rieger, B. 2-Methoxyethylamino-Bis(Phenolate)Yttrium Catalysts for the Synthesis of Highly Isotactic Poly(2-Vinylpyridine) by Rare-Earth Metal-Mediated Group Transfer Polymerization. *Macromolecules* **2016**, 49 (17), 6260–6267.
- (93) Masamune, S.; Choy, W.; Petersen, J. S.; Sita, L. R. Double Asymmetric Synthesis—a New Strategy for Stereochemical Control in Organic Synthesis. *Angew. Chem., Int. Ed. Engl.* **1985**, 24 (1), 1–76.
- (94) Evans, D. A.; Miller, S. J.; Lectka, T.; von Matt, P. Chiral Bis(Oxazoline)Copper(II) Complexes as Lewis Acid Catalysts for the Enantioselective Diels—Alder Reaction. *J. Am. Chem. Soc.* **1999**, *121* (33), 7559—7573.
- (95) Duplantier, A. J.; Nantz, M. H.; Roberts, J. C.; Short, R. P.; Somfai, P.; Masamune, S. Triple Asymmetric Synthesis for Fragment Assembly: Validity of Approximate Multiplicativity of the Three Diastereofacial Selectivities. *Tetrahedron Lett.* **1989**, 30 (52), 7357–7360.
- (96) Crowden, C. J.; Paterson, I. Asymmetric Aldol Reactions Using Boron Enolates. *Org. React.* **1997**, *51*, 1–200.

- (97) Wan, Z.-K.; Choi, H.; Kang, F.-A.; Nakajima, K.; Demeke, D.; Kishi, Y. Asymmetric Ni(II)/Cr(II)-Mediated Coupling Reaction: Stoichiometric Process. *Org. Lett.* **2002**, *4* (25), 4431–4434.
- (98) Choi, H.; Nakajima, K.; Demeke, D.; Kang, F.-A.; Jun, H.-S.; Wan, Z.-K.; Kishi, Y. Asymmetric Ni(II)/Cr(II)-Mediated Coupling Reaction: Catalytic Process. *Org. Lett.* **2002**, *4* (25), 4435–4438.